Pulsed EM Field Radio

The Low-Power, Ultra-fast Bridge to Ubiquitous Fiber Networks

Lager, Ioan; Zito, Domenico

Publication date
2019

Document Version
Final published version

Published in
2019 13th European Conference on Antennas and Propagation (EuCAP)

Pulsed EM Field Radio: The Low-Power, Ultra-fast Bridge to Ubiquitous Fiber Networks

Ioan E. Lager[#1], Domenico Zito[*2]

[#]Faculty of Electrical Engineering, Mathematics and Computer Science, Delft University of Technology, the Netherlands
[*]Department of Engineering - Electrical and Computer Engineering, Aarhus University, Denmark.
[1]i.e.lager@tudelft.nl, [2]domenico.zito@eng.au.dk

***Abstract* — The suitability of pulsed electromagnetic (EM) field radio as a low-power, ultra-fast instrument for bridging the gap between mobile terminals and ubiquitously deployed fiber-optic networks is investigated. An in-depth study of the present trends in fifth generation (5G) mobile communications strategies is carried out, by highlighting the crucial role of Terahertz (THz) and 'low-GHz' ultra-wideband (UWB) radio implementations. Upon recognising the low-power capabilities of 'low-GHz' UWB solutions, the contribution zooms in on the pulsed EM field transfer and on the features of a monocycle pulse generator that is deemed conditional for future physical realisations of the concept.**

***Keywords* — baseband digital communication, time-domain electromagnetics, pulse circuits.**

I. Introduction

The fifth generation (5G) mobile communications is expected to commence initial commercialisation in 2020. 5G is credited with enticing capabilities, such as (ultra-)high data rate, low latency and massive connectivity, and is poised to open unprecedented societal and commercial opportunities.

Despite the implementation of (pre-)5G connectivity being almost taken for granted, there are still important technological challenges ahead, and intense research is currently invested in removing these roadblocks. This contribution will perform an in-depth study of the current status and developments in this field, and examine in detail the decisive *physical layer instruments* to ensuring the throughput that is commonly associated with 5G. The study will start by analysing the present trends at the lowest 3 layers of the Open Systems Interconnection (OSI) reference model [1], as reflected in very recent literature sources. This survey will allow conjecturing the benefits of using pulsed electromagnetic (EM) field wireless transfer as a means for bridging the 'last centimetres' between mobile terminals and a ubiquitously deployed fiber-optic network. The next step will elaborate upon a baseband transmitter making use of a solid-state, nanosecond, monocycle generator with unique specifications, by also highlighting its congruence with theoretical results in time-domain (TD) electromagnetics. The survey will end by drawing conclusions.

II. New Radio: a paradigm change in wireless connectivity

A. Architectures & protocols

Providing 5G services requires reconsidering the very foundations of (cellular) mobile networks, a fact reflected in 5G networks being often referred to as *New Radio* – a term that is gaining momentum in the communication community. For example, [2] defines "New Radio" in terms of delivered peak data rate, user experienced data rate (interestingly enough, a performance indicator whose relevance was already anticipated in [3]), area traffic capacity, latency, energy efficiency, reliability, mobility, bandwidth and support of a wide range of services. Furthermore, [4] highlights the crucial role played by efficient and flexible use of spectrum in 5G (see also [5] for the current status and the challenges ahead in spectrum use). Supplying the pledged 5G data rate is only conceivable in smaller and smaller cells, with *ultra-dense cellular networks* being increasingly investigated at the conceptual and protocol levels [6] (note, however, that [7] already warned about the limits of densification being close to being reached, at least with the wireless technologies currently in use). To conclude with, *caching* is envisaged as a critical enabler for providing ultra-high throughput, the opportunities of this technique being analysed in [8], and its potential caveats in [9].

B. Wireless technologies

The strategies catalogued in Section II-A concentrate on the network architectures and protocols, with little more than general references to their actual physical implementation.

Upon recognising that data-rate is conditioned by channel bandwidth, most authors advocate a push towards higher frequencies, with Terahertz (THz) technology (with carriers in the hundreds of GHz) being largely believed to be the ultimate solution. For example [10] discusses the high promises for wireless backhaul and wireless local access of a THz baseband fiber-to-wireless interface (the paper remaining at a rather abstract level). However, free-space THz propagation is impeded upon by large spreading loss and molecular absorption [11] (this paper proposing a distance-aware, physical-layer design with massive multiple-input, multiple-output (MIMO) as a feasible countermeasure). Another important roadblock in THz communications is the so-called *THz gap*[†] that drastically limits the available power, especially (well) above 100 GHz, with [12] presenting illustrative measurements – here, [13] may offer the needed breakthrough in sidestepping the THz gap. As a result, although long-range, backhaul connections are also

[†]As stated in [12], the THz frequency range envisaged for communications (in the hundreds of GHz spectrum) is too high for using regular oscillators and too low for using optical photon emitters as signal generators.

reported in the literature [14], the combination of pass-loss and limited power availability recommends the use of THz wireless solutions for short-range communications. A suchlike example is the "fly's eye spherical antenna" concept [15], promising 12 Tb/s throughput via a frequency reuse scheme in a spectrum around 120 GHz. Alternatively, [12] advocates a 'last metre' indoor THz wireless access and provides measurement evidence of its feasibility (nonetheless, without giving indications on the physical implementation of such a system).

The alternative for providing the needed bandwidth is the ultra-wideband (UWB) technology in the 'low-GHz' spectrum. Immediately after the release by the Federal Communications Commission (FCC) of the $3.1 \div 10.6$ GHz UWB band [16] there was a surge in investigations concerning UWB wireless communication systems, with [17] giving a broad overview of the potential application opportunities. However, these designs proved of little practical use due to the drastic radiated power limitations of the FCC mask and, even more importantly, due to the non-uniform UWB band definitions in different geographic areas. As a result, few (if any) viable commercial solutions emerged. Despite these setbacks, distinctive prospects, such as combined communication and localisation [18], [19] and, especially, low-power operation – a critical enabler for developing energetically self-reliant devices [20], [21], maintained a constant (somehow academic) interest for UWB technology. The combination of large throughput and low-power operation was used in [3] for justifying the opportunity of 'low-GHz' UWB radio for *very-short range*, (ultra-)fast transfer and, recently, [4] reiterated that UWB radio is the path towards ensuring power-efficiency, capacity and coverage in 5G networks.

C. Ultra-fast indoor communication

The argumentation above highlighted that both THz and 'low-GHz' UWB technologies are exceptionally suitable for short-range communications. Suchlike communications are of particular importance for (ultra-fast) indoor communication. Recent developments in optics and photonics [22] have opened new avenues towards photonic home area networks [23], especially via low-cost plastic optical fiber [24]. With fiber-optic connectivity becoming ubiquitous, the challenge is now to wirelessly connect to a myriad of photonic access points within reach, this amounting to bridging the 'last meter' or even the 'last centimetres'. Two viable solutions to this end were proposed in [12] (THz technology) and [3] (UWB, near-field, wireless plug-in), the latter also (presumably) ensuring low-power operation. Note that indoor communication bears similarities with the KIOSK data downloading that was initially proposed in [17] (UWB implementation), and revisited in [3] (again UWB) and [25] (THz implementation). As a final remark, both indoor communication and KIOSK data downloading can benefit a lot from intelligent data caching.

D. Pulsed-field radio – an overview

The benefits of UWB radio are fully exploited in a pulsed EM field transfer scenario with the following features: (i) a baseband (carrier-free) channel making use of simple coding schemes; (ii) very-short range ($\approx$ centimetres), entirely falling within the near-field zone of the transmitter (see [26] for the applicable definitions); (iii) radiated power levels far under the FCC mask for allowing license-free operation.

The implementation of such a transfer hinges on progress at the level of antenna front-ends and, above all, on the availability of high-quality, solid-state, low-power, pulse generating circuitry. With reference to such generators, it is noted that early implementation were demonstrated in [27], [28] and, subsequently, in [29] (in conjunction with fiber optics). However, what was needed were nanosecond monocycle generators, with [30], [31] providing for the first time the needed functionality. An improved variant of the circuit discussed in [31] was later shown in [32], that implementation representing, to the authors' best knowledge, the best solid-state monocycle generator reported in the literature to-date. Consequently, the circuit reported in [32] is deemed optimally placed for implementing a pulsed EM field 'last centimetre' wireless link featuring ultra-fast (above 3 Gb/s) throughput, under severe power consumption limitations. For implementing the full channel, the pulse generator must be complemented by UWB/baseband receivers/transceivers (here [33]–[35] offer interesting solutions). To conclude with, for further curbing the power consumption, the channel coding should be as simple as possible, [36] giving relevant guidelines to this end.

III. Monocycle pulse generator

A. Monocycle pulse generator: implementation and key performance indicators

On-chip pulse generation is challenging [32], as achieving pulses with a desired form factor, a very short duration and an adequate amplitude is conditioned by fundamental technological limits. In [31], a very effective pseudo-gaussian monocycle pulse generator designed in 90 nm, bulk complementary metaloxidesemiconductor (CMOS) technology was introduced and demonstrated experimentally. In [32], the opportunity offered by this solution has been pushed further to the 28 nm, fully-depleted, silicon-on-insulator (FDSOI) CMOS technology, this yielding monocycle pulses with a peak-to-peak amplitude of 1.18 V and a duration of 70 ps. Details on the key features are available in [32] and thereby will not be repeated here.

In the interest of the reader, it is worth briefly explaining that the pulse generator (see Fig. 1) consists of two triangular pulse generators (TPGs), a delay element (t) and a shaping network (SN). The operating principle consists of overdriving the common-source differential pair (*i.e.*, SN) by means of two triangular monocycle pulses, the second pulse delayed by its duration time. At each occurrence of the negative edge of the command control signal, the pulse generator provides a monocycle pulse, as shown in Fig. 2.a. Note that, considering a one-bit pulse polarity coding, theoretical data-rates in excess of 10 Gb/s can be achieved with such a short pulse. Furthermore, Fig. 2.b shows the spectral density per single pulse, which exhibits a peak of -125 dBm/MHz at about 14 GHz.

Despite being a side-effect, it is mentioned that the initial down-wiggle in Fig. 2.a is a simulation artifact and is due to the

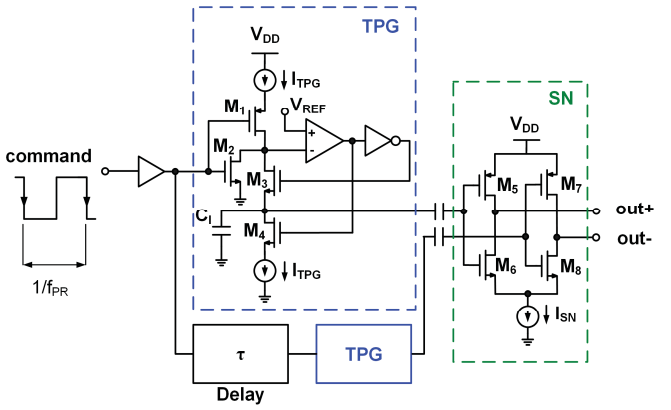

Fig. 1. Schematic of the pulse generator discussed in [32]. TPG = triangular pulse generators; SN = the shaping network.

combined effect of fast digital command signal switching and residual charge redistribution through C_l and the decoupling capacitances at the input of the shaping network. However, due to the finite resistance of interconnects, this effect will not occur in an actual physical implementation on silicon.

B. *Mathematical replication of generate monocycle pulse*

As stated in Section II-D, the monocycle pulse generator presented above is an excellent candidate for implementing a pulsed EM field, 'last centimetre' wireless link. It will now be shown how the generated waveform fits in the theoretical framework at the core of the pulsed, near-field EM transfer.

The radiation from a CMOS embedded pulse-fed loop antenna was theoretically studied in [37]. In that paper it was stressed the importance of the feeding pulse (i) being *causal* and (ii) having an analytical expression that is controllable via a reduced number of parameters. The excitation used in [37] had the shape of a time-differentiated, power exponential pulse [38]. While being causal, such a pulse has a, theoretically, infinite tail, making it less adequate for high pulse repetition rates, as required by ultra-fast communications. To address this issue, [39] introduced the windowed-power (WP) family of pulses with a finite temporal support.

The signature in Fig. 2.a will be shown to be in excellent agreement with the time-differentiated, WP pulse $\partial_t \mathrm{WP}(\nu, t)$. To this end, the part of the plot in between the cyan and light-red boxes[‡] is firstly clipped out and time-shifted to $t = 0\,\mathrm{ns}$. Applying the replication strategy described in [39, Section V.B] to this signature yields a $\partial_t \mathrm{WP}(\nu, t)$ pulse having the parameters: raising power $\nu = 4$, pulse rise-time $t_\mathrm{r} = 37\,\mathrm{ps}$ and amplitude $V_0 = 0.59\,\mathrm{V}$ (see [39] for the relevant definitions). The original $p(t)$ (the initial down-wiggle included) and the pulse replica signatures are shown in Fig. 3.a. The deviation

[‡]The $\partial_t \mathrm{WP}(\nu, t)$ cannot replicate the down-wiggle preceding the pulse onset. Furthermore, the part of the pulse marked by the light-red box is, for all practical purposes, zero and needs not being replicated.

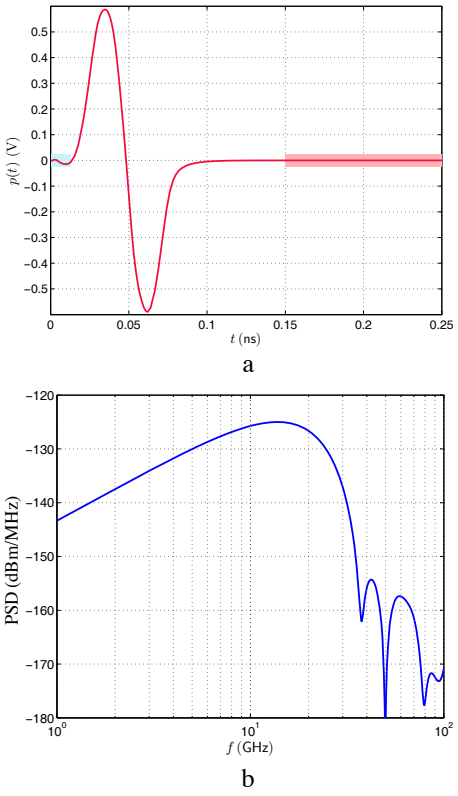

Fig. 2. Original $p(t)$ pulse reported in [32] – single-pulse operation. (a) Time-domain signature; the light-cyan box designates the initial down-wiggle in the measured signature, and the light-red box designates the zero tail (inter-pulse guard in [32]); (b) spectral content; note that the spectral diagrams reported in [32] corresponded to a 1 MHz pulse repetition rate.

between the two signatures is calculated with the expression

$$\mathrm{ERR}_{\%}(\nu) = \frac{\int_{t=0}^{t=t_\mathrm{f}} \left[\partial_t \mathrm{WP}(\nu, t) - p(t)\right]^2 \mathrm{d}t}{\int_{t=0}^{t=t_\mathrm{f}} p^2(t)\mathrm{d}t} 100 \qquad (1)$$

in which t_f is taken just after the $\partial_t \mathrm{WP}(\nu, t)$ pulse's support. In the case of the constructed replica, this deviation amounts to 0.22% when excluding the initial down-wiggle in $p(t)$, and to 0.25% when considering it. The spectral contents of the $\partial_t \mathrm{WP}(\nu, t)$ replica is shown in Fig. 3.b, this plot accurately reproducing the main features of the spectrum in Fig. 2.b.

The pulse $p(t)$ was also replicated by using a raising power $\nu = 5$, a choice ensuring a smooth open-circuit (Thévenin) induced voltage in a loop-to-loop transfer (see Eq. (9) in [40]). The corresponding parameters were in this case: $\nu = 5$, $t_\mathrm{r} = 41\,\mathrm{ps}$ and $V_0 = 0.59\,\mathrm{V}$, the TD comparison of the original $p(t)$ and its replica being illustrated in Fig. 4.a. The corresponding deviations calculated via (1) are 0.46% (no down-wiggle) and 0.48% (global) – still an excellent congruence! As expected, the spectral content (shown in Fig. 4.b) is also in very good agreement with that in Fig. 2.b.

It can now be concluded that the suitability of the monocycle generated by the circuit proposed in [32] was also cogently demonstrated from a theoretical, EM perspective. That pulse is

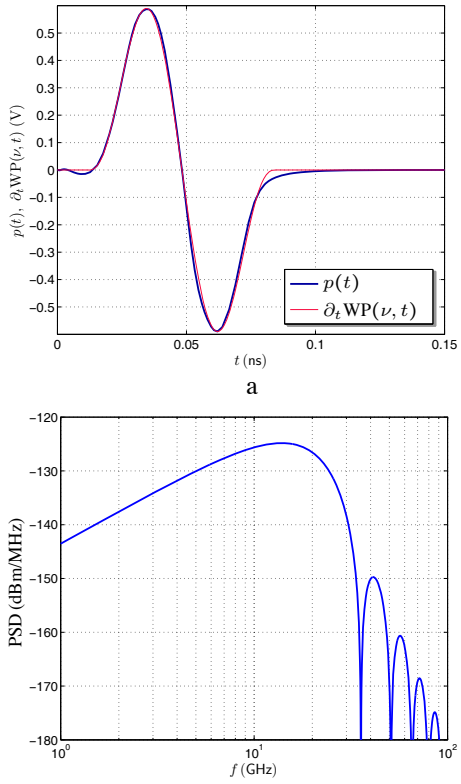

Fig. 3. Original $p(t)$ pulse and its $\partial_t \mathrm{WP}(\nu,t)$ replica for ν = 4. (a) Comparison of time-domain signatures; (b) spectral content of $\partial_t \mathrm{WP}(\nu,t)$.

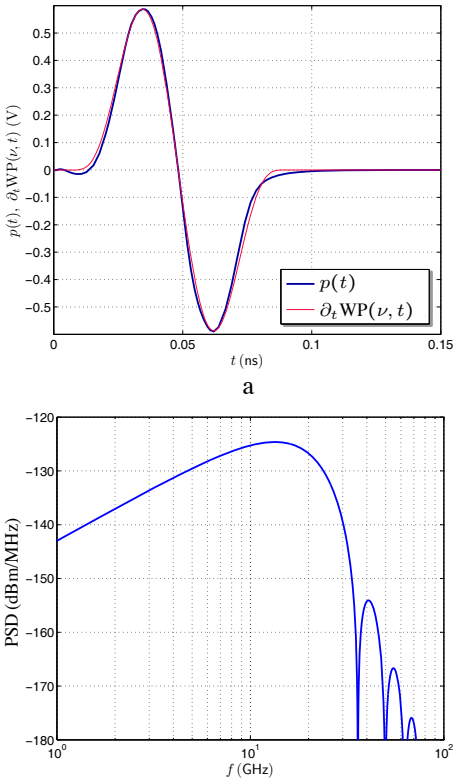

Fig. 4. Original $p(t)$ pulse and its $\partial_t \mathrm{WP}(\nu,t)$ replica for ν = 5. (a) Comparison of time-domain signatures; (b) spectral content of $\partial_t \mathrm{WP}(\nu,t)$.

causal, is time-windowed and offers the smoothness required for an adequate implementation of a loop-to-loop transfer.

As a final remark, it is mentioned that the exceptional analytic features of the generated monocycle may also serve a purpose in a TD imaging technique for shape reconstruction of impenetrable and penetrable objects [41], this opportunity being currently investigated.

IV. Conclusions

The suitability of pulsed EM field radio as a low-power, ultra-fast instrument for bridging the 'last centimetres' between mobile terminals and the photonic access points to a ubiquitously deployed fiber-optic network was investigated. This suitability was substantiated by firstly presenting a broad overview of the present trends in 5G mobile communications strategies. Upon singling out the THz technology and the 'low-GHz' ultra-wideband (UWB) radio implementations as the paths to be followed, the account focused on the latter as the solution to combining the needed throughput with the (ultra-)low power operation that is indispensable to any mobile device implementation. To this end, the account put forward a monocycle pulse generator realised in the 28 nm, FDSOI, CMOS technology as a key enabler for implementing a 'last centimetre' wireless link. That chip is capable of delivering monocycle pulses with a peak-to-peak amplitude of 1.18 V and a duration of 70 ps. It was stated that, in the case a close-range, pulsed EM field transfer using a one-bit pulse polarity coding, the generated pulses can yield theoretical data-rates in excess of 10 Gb/s. Those pulses were also shown to have exceptional analytical properties, as they represent an almost exact replica of a causal pulse with finite temporal support (a $\partial_t \mathrm{WP}(\nu,t)$ pulse) featuring the smoothness needed in a loop-to-loop, pulsed EM field transfer.

Acknowledgment

The authors hereby acknowledge the suggestion received from Dr. Martin Štumpf about the suitability of the monocycle generated by the circuit in [32] to TD imaging techniques.

References

[1] H. Zimmermann, "OSI reference model – The ISO model of architecture for open systems interconnection," *IEEE Trans. Commun.*, vol. 28, no. 4, pp. 425–432, Apr. 1908.

[2] J. Jeon, "NR wide bandwidth operations," *IEEE Commun. Mag.*, vol. 56, no. 3, pp. 42–46, Mar. 2018.

[3] I. E. Lager, R. B. Staszewski, A. B. Smolders, and D. M. W. Leenaerts, "Ultra-high data-rate wireless transfer in a saturated spectrum – new paradigms," in *Proc. 44^{th} EuMC*, 2014, pp. 917–920.

[4] J. J. Gimenez, D. Gomez-Barquero, J. Morgade, and E. Stare, "Wideband broadcasting: A power-efficient approach to 5G broadcasting," *IEEE Commun. Mag.*, vol. 56, no. 3, pp. 119–125, Mar. 2018.

[5] J. Lee, E. Tejedor, K. Ranta-aho, H. Wang, K.-T. Lee, E. Semaan, E. Mohyeldin, J. Song, C. Bergljung, and S. Jung, "Spectrum for 5G: Global status, challenges, and enabling technologies," *IEEE Commun. Mag.*, vol. 56, no. 3, pp. 12–18, Mar. 2018.

[6] M. Gao, J. Li, D. N. K. Jayakody, H. Chen, Y. Li, and J. Shi, "A super base station architecture for future ultra-dense cellular networks: Toward low latency and high energy efficiency," *IEEE Commun. Mag.*, vol. 56, no. 6, pp. 35–41, Jun. 2018.

[7] J. G. Andrews, X. Zhang, G. D. Durgin, and A. K. Gupta, "Are we approaching the fundamental limits of wireless network densification?," *IEEE Commun. Mag.*, vol. 54, no. 10, pp. 184–190, Oct. 2016.

[8] D. Liu, B. Chen, C. Yang, and A. F. Molisch, "Caching at the wireless edge: Design aspects, challenges, and future directions," *IEEE Commun. Mag.*, vol. 54, no. 9, pp. 22–28, Sep. 2016.

[9] G. Paschos, E. Bastug, I. Land, G. Caire, and M. Debbah, "Wireless caching: Technical misconceptions and business barriers," *IEEE Commun. Mag.*, vol. 54, no. 8, pp. 16–22, Aug. 2016.

[10] A.-A. A. Boulogeorgos, A. Alexiou, T. Merkle, C. Schubert, R. Elschner, A. Katsiotis, P. Stavrianos, D. Kritharidis, P.-K. Chartsias, J. Kokkoniemi, M. Juntti, J. Lehtomaki, A. Teixeira, and F. Rodrigues, "Terahertz technologies to deliver optical network quality of experience in wireless systems beyond 5G," *IEEE Commun. Mag.*, vol. 56, no. 6, pp. 144–151, Jun. 2018.

[11] I. F. Akyildiz, C. Han, and S. Nie, "Combating the distance problem in the millimeter wave and terahertz frequency bands," *IEEE Commun. Mag.*, vol. 56, no. 6, pp. 102–108, Jun. 2018.

[12] V. Petrov, J. Kokkoniemi, D. Moltchanov, J. Lehtomaki, Y. Koucheryavy, and M. Juntti, "Last meter indoor terahertz wireless access: Performance insights and implementation roadmap," *IEEE Commun. Mag.*, vol. 56, no. 6, pp. 35–41, Jun. 2018.

[13] A. Garufo, G. Carluccio, N. Llombart Juan, A. Neto, and I. E. Lager, "Analysis of photoconductive antenna power radiation by Norton equivalent circuit," in *Proc. 47^{th} EuMC*, 2017, pp. 268–271.

[14] S. Koenig, D. Lopez-Diaz, J. Antes, F. Boes, R. Henneberger, A. Leuther, A. Tessmann, R. Schmogrow, D. Hillerkuss, R. Palmer, T. Zwick, C. Koos, W. Freude, O. Ambacher, J. Leuthold, and I. Kallfass, "Wireless sub-THz communication system with high data rate," *Nature Photonics* vol. 7, pp. 977–981, Dec. 2013. [Online]. doi: 10.1038/NPHOTON.2013.275.

[15] N. Llombart, D. Emer, M. Arias, and E. McCune, "Fly's eye spherical antenna system for future Tbps wireless communications," in *Proc. 11^{th} EuCAP*, 2017, pp. 1659–1662.

[16] Federal Communications Commission, "First Report and Order," April 2002.

[17] D. Porcino and W. Hirt, "Ultra-wideband radio technology: Potential and challenges ahead," *IEEE Commun. Mag.*, vol. 41, no. 7, pp. 66–74, Jul. 2003.

[18] H. Lücken, *Communication and Localization in UWB Sensor Networks. A Synergetic Approach*, PhD dissertation No. 20776, ETH Zürich, 2012. [Online]. Available: http://e-collection.library.ethz.ch/view/eth:6540.

[19] H. Luecken, C. Steiner, and A. Wittneben, "Location-aware UWB communication with generalized energy detection receivers," *IEEE Trans. Wireless Commun.*, vol. 11, no. 9, pp. 3068–3078, Sept. 2012.

[20] R. Dokania, X. Wang, S. Tallur, C. Dorta-Quinones, and A. Apsel, "An ultralow-power dual-band UWB impulse radio," *IEEE Trans. Circuits Syst. II, Exp. Briefs*, vol. 57, no. 7, pp. 541–545, Jul. 2010.

[21] M. Gorlatova, *Energy Harvesting Networked Nodes: Measurements, Algorithms, and Prototyping*, PhD dissertation, NY: New York, Columbia University, 2013. [Online]. Available: http://academiccommons.columbia.edu/item/ac:161643.

[22] A. E. Willner, R. L. Byer, C. J. Chang-Hasnain, S. R. Forrest, H. Kressel, H. Kogelnik, G. J. Tearney, C. H. Townes, and M. N. Zervas, "Optics and photonics: Key enabling technologies," *Proc. IEEE*, vol. 100, pp. 1604–1643, May. 2012.

[23] A. M. J. Koonen, Fellow and E. Tangdiongga, "Photonic home area networks," *J. Light. Technol.*, vol. 32, no. 4, pp. 591–604, Feb. 2014.

[24] Y. Shi, E. Tangdiongga, A. M. J. Koonen, A. Bluschke, P. Rietzsch, J. Montalvo, M. M. de Laat, G. N. van den Hoven, and B. Huiszoon, "Plastic-optical-fiber-based in-home optical networks," *IEEE Commun. Mag.*, vol. 52, no. 6, pp. 186–193, Jun. 2014.

[25] H.-J. Song, H. Hamada, and M. Yaita, "Prototype of KIOSK data downloading system at 300 GHz: Design, technical feasibility, and results," *IEEE Commun. Mag.*, vol. 56, no. 6, pp. 130–136 , Jun. 2018.

[26] I. E. Lager and A. B. Smolders, "On the adequacy of the far-field conditions for pulsed radiated EM fields," *IEEE Antennas Wireless Propag. Lett.*, vol. 14, pp. 1561–1564, Aug. 2015.

[27] R. J. Fontana, "Recent system applications of short-pulse ultra-wideband (UWB) technology," *IEEE Trans. Microw. Theory Techn.*, vol. 52, no. 9, pp. 2087–2014, Sep. 2004

[28] R. C. Qiu, H. Liu, and X. Shen, "Ultra-wideband for multiple access communications," *IEEE Commun. Mag.*, vol. 43, no. 2, pp. 80–87, Feb. 2005.

[29] T. B. Gibbon, X. Yu, R. Gamatham, N. Guerrero Gonzalez, R. Rodes, J. Bevensee Jensen, A. Caballero, and I. T. Monroy, "3.125 Gb/s impulse radio ultra-wideband photonic generation and distribution over a 50 km fiber with wireless transmission," *IEEE Microw. Wireless Compon. Lett.*, vol. 20, no. 2, pp. 127–129, Feb. 2010.

[30] M. Hafiz, S. Kubota, N. Sasaki, K. Kimoto, and T. Kikkawa, "A 2 Gb/s 1.8 pJ/bit differential BPSK UWB-IR transmitter using 65 nm CMOS technology," *IEICE Trans. Electron.*, vol. E94-C, no. 2, pp. 977–984, Feb. 2011.

[31] F. Zito, D. Pepe, and D. Zito, "UWB CMOS monocycle pulse generator," *IEEE Trans. Circuits Syst. I, Reg. Papers*, vol. 57, no. 10, pp. 2654–2664, Oct. 2010.

[32] D. Pepe, L. Aluigi, and D. Zito, "Sub-100 ps monocycle pulses for 5G UWB communications," in *Proc. 10^{th} EuCAP*, 2016, pp. 1–4.

[33] F. Zhang, A. Jha, R. Gharpurey, and P. Kinget, "An agile, ultra-wideband pulse radio transceiver with discrete-time wideband-IF," *IEEE J. Solid-State Circuits*, vol. 44, no. 5, pp. 1336–1351, May 2009.

[34] T. Maehata, S. Kameda, and N. Suematsu, "High ACLR 1-bit direct radio frequency converter using symmetric waveform," in *Proc. 42^{nd} EuMC*, Amsterdam, the Netherlands, Oct.-Nov. 2012, pp. 1051–1054.

[35] S. Palermo, S. Hoyos, A. Shafik, E. Z. Tabasy, S. Cai, S. Kiran, and K. Lee, CMOS ADC-based receivers for high-speed electrical and optical links *IEEE Commun. Mag.*, vol. 54, no. 10, pp. 168–175, Oct. 2016.

[36] H. Ruotsalainen, N. Leder, B. Pichler, H. Arthaber, and G. Magerl, "Equivalent complex baseband model for digital transmitters based on 1-bit quadrature pulse encoding," *IEEE Trans. Circuits Syst. I, Reg. Papers*, vol. 62, no. 11, pp. 2739–2747, Nov. 2015.

[37] I. E. Lager, V. Voogt, and B. J. Kooij, "Pulsed EM field, close-range signal transfer in layered configurations – a time-domain analysis," *IEEE Trans. Antennas Propag.*, vol. 62, no. 5, pp. 2642–2651, May 2013.

[38] I. E. Lager, A. T. de Hoop, and T. Kikkawa, "Model pulses for performance prediction of digital microlectronic systems," *IEEE Trans. Compon., Packag., Manuf. Technol.*, vol. 2, no. 11, pp. 1859–1870, Nov. 2012.

[39] I. E. Lager and S. L. van Berkel, "Finite temporal support pulses for EM excitation," *IEEE Antennas Wireless Propag. Lett.*, vol. 16, pp. 1659–1662, Jun. 2017.

[40] I. E. Lager and A. T. de Hoop, "Loop-to-loop pulsed electromagnetic field wireless signal transfer," in *Proc. 6^{th} EuCAP*, 2012, pp. 786–790.

[41] M. Štumpf, "Radar imaging of impenetrable and penetrable targets from finite-duration pulsed signatures," *IEEE Trans. Antennas Propag.*, vol. 62, no. 6, pp. 3035–3042, June. 2014.